HHS Public Access

Author manuscript

Bioorg Med Chem Lett. Author manuscript; available in PMC 2022 February 16.

Published in final edited form as:

Bioorg Med Chem Lett. 2020 June 01; 30(11): 127162. doi:10.1016/j.bmcl.2020.127162.

Design, synthesis and biological evaluation of spiropyrazolopyridone derivatives as potent dengue virus inhibitors

Jimin Xu[a,†], **Xuping Xie**[b,†], **Haiying Chen**[a], **Jing Zou**[b], **Yu Xue**[a], **Na Ye**[a], **Pei-Yong Shi**[b,c,*], **Jia Zhou**[a,c,*]

[a]Chemical Biology Program, Department of Pharmacology and Toxicology, University of Texas Medical Branch, Galveston, Texas 77555, United States

[b]Department of Biochemistry and Molecular Biology, University of Texas Medical Branch, Galveston, Texas 77555, United States

[c]Sealy Center for Structural Biology and Molecular Biophysics, University of Texas Medical Branch, Galveston, Texas 77555, United States

Abstract

The effective treatment for dengue virus infection continues to be a challenge. We herein reported our continued SAR exploration on the spiropyrazolopyridone scaffold. Introducing different substituents at the 3′- or 5′-site of the pyrazolopyridone core or moving the benzyl chain to the adjacent nitrogen led to a significant loss of potency on DENV-2. While a narrow range of substitutions were tolerated at the *para*-position of the phenyl ring, di-substitution on the phenyl ring is beneficial for DENV-2 potency and has variable influences on DENV-3 potency depending on the exact compound. Among these molecules, compounds **22** (**JMX0376**) with 4-chloro-3-fluorobenzyl and **24** (**JMX0395**) with 2,4-bis(trifluoromethyl)benzyl showed the most potent and broadest inhibitory activities against DENV-1 to -3 with nanomolar to low micromolar EC_{50} values.

Graphical Abstract

*Corresponding authors. Jia Zhou, Tel.: +1-409-772-9748; fax: +1-409-772-9648; jizhou@utmb.edu. Pei-Yong Shi, Tel.: +1-409-772-6370; fax: +1-409-772-4298; peshi@utmb.edu.
†These authors contributed equally to the manuscript.

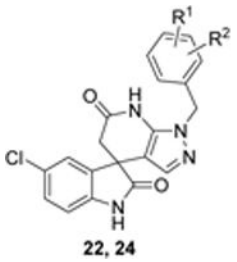

22, 24

22 (JMX0376)	24 (JMX0395)
R^1, R^2 = 4-chloro-3-fluoro	R^1, R^2 = 3,5- bis(trifluoromethyl)
DENV-1 EC_{50} = 1.8 μM	DENV-1 EC_{50} = 1.6 μM
DENV-2 EC_{50} = 0.050 μM	DENV-2 EC_{50} = 0.038 μM
DENV-3 EC_{50} = 0.019 μM	DENV-3 EC_{50} = 0.017 μM
DENV-4 EC_{50} > 5 μM	DENV-4 EC_{50} > 5 μM
CC_{50} > 10 μM	CC_{50} > 10 μM

Keywords

Dengue virus; Spiropyrazolopyridone; NS4B inhibitors; Antiviral agents; Structure-activity relationship (SAR)

Dengue is a febrile disease that is caused by any one of the four closely related serotypes of dengue viruses (DENV-1, -2, -3 and -4) with asymptomatic, mild or severe symptoms. Common symptoms are flu-like with patients experiencing high fever, headaches, retro-orbital pain, joint/bone/muscle pain, vomiting, rash and fatigue. In most cases, DENV infection is self-limiting, but sometimes it can develop into life-threatening illnesses, dengue hemorrhagic fever (DHF) or dengue shock syndrome (DSS).[1] Dengue has become a major public health threat throughout tropical and sub-tropical regions of the world, putting about 3.9 billion people in 128 countries at risk.[2, 3] Over the past 50 years, there is an unprecedented increase in the incidence of dengue and 390 million people are estimated to get infected with dengue annually, 96 million of which experience clinical symptoms (with any severity of disease), including 500,000 cases of severe dengue and 22,000 deaths worldwide.[4–6] Infection confers life-long immunity to that particular serotype while cross-immunity against other serotypes is only partial and temporary.[7, 8] However, a second infection with a different DENV increases the probability of severe dengue through a process known as antibody-dependent enhancement (ADE).[9–12] As a result, an ideal dengue antiviral or vaccine should be equally effective against all four DENV serotypes. Recently, the first dengue vaccine (CYD-TDV from Sanofi Pasteur) has been approved by regulatory authorities in about 20 countries with limited efficacy and safety issues.[13–15] It requires a three-dose regimen and is targeted for persons aged 9–45 years old who were previously infected by DENV. Moreover, according to the recommendations of World Health Organization (WHO) regarding the use of CYD-TDV in September 2018, seronegative vaccine recipients suffer an excess risk of hospitalized and severe dengue compared to seronegative unvaccinated individuals.[16] While numerous efforts were made towards anti-dengue drug discovery by different research groups, there remains no specific therapy for dengue illness.[17] Therefore, there remains an urgent need to develop effective and safe antiviral agents for the treatment of dengue infections.

Through a DENV-2 high-throughput phenotypic screening, spiropyrazolopyridone **1** (Figure 1) was identified as a novel potent DENV inhibitor.[18–20] The *R* enantiomer **1a** was then separated by chiral high-performance liquid chromatography (HPLC) and confirmed to be far more potent than the corresponding *S* enantiomer of racemate **1**. Genetic analysis showed that mutations in DENV-2 NS4B conferred resistance to compound **1a** inhibition,

suggesting that this class of compounds likely targets viral NS4B protein. To improve the physicochemical properties, compound **2** with 3-pyridyl was discovered with good *in vivo* pharmacokinetic profiles and efficacy in DENV-2 infected AG129 mice. However, this class of compounds lacks potency against DENV-1 and DNEV-4. Our group previously directed the structure-activity relationship (SAR) exploration mainly on the amide of the indolone moiety of this series and found that a wide range of substitutions were well tolerated at this position. Compound **3** with an isopentyl chain showed the most potent and broadest inhibitory activities, effective against DENV-1 to -3 with nanomolar to submicromolar EC_{50} values, while exhibiting promising efficacy in the A129 mouse models.[21] These good *in vivo* results suggest that this spiropyrazolopyridone scaffold is worthy of further optimization efforts to elucidate the chemical space for the potential to identify pan-serotype DENV inhibitors. As part of our ongoing antiviral drug discovery and development program,[21–26] we herein report our continued SAR investigation of this series, mainly focused on the pyrazolopyridone moiety.

Previous studies showed a narrow range of *para*-substitutions were tolerated on the phenyl ring while *meta*- or *ortho*-substitutions resulted in a significant loss of potency on DENV-2.[18] Based on these results, we first attempted to introduce different functional groups at the *para*-position and investigated the effect of di-substitutions on the phenyl ring as well. Compounds **16-24** were prepared as outlined in Scheme 1. Substitution of 3-aminopyrazole with different substituted benzyl bromide or benzyl chloride afforded the final products as two isomers, which were then successfully separated by column chromatography to give 1-benzyl-5-aminopyrazole derivatives **5a-13a**. The subsequent three component condensation of aminopyrazoles **5a-13a**, 5-chloroisatin and Meldrum's acid provided a series of spiropyrazolopyridone analogues **16-19** and **21-24**.[27] Acid analogue **20** was accessed from ester **19** via hydrolysis. As shown in Table 1, 4-flurobenzyl substitution (**16**) resulted in a significant loss of potency against DENV-2 (EC_{50} = 4.2 μM), while functional groups cyano (**17**), sulfonyl (**18**), ester (**19**) and acid (**20**) on the para-position of the phenyl ring were all unfavorable for potency, not effective against DENV-2 up to 5 μM.[28] These results are consistent with the trend observed before. Interestingly, di-substitutions analogues **21–24** displayed similar or improved potency against DNEV-2 compared to mono-substitution analogue **1**. Compound **21** with 3,4-dichlorobenzyl exhibited improved potency against DENV-1 and DENV-2 (EC_{50} = 1.8 μM and 0.062 μM, respectively) meanwhile displaying a dramatic loss of potency against DENV-3 (EC_{50} > 5 μM). Remarkably, replacing 3-Cl with 3-F (**22**) maintained the same level of potency against DENV-1 (EC_{50} = 1.8 μM) and DENV-2 (EC_{50} = 0.019 μM), while it regained potent activity against DENV-3 with an EC_{50} value of 0.019 μM as compared with compound **21**. Moving the 3-F group to the ortho position (**22**) resulted in a 20-fold loss of potency against DENV-3 (EC_{50} = 0.39 μM) and slightly decreased activities against DENV-1 (EC_{50} = 2.3 μM) and DENV-2 (EC_{50} = 0.14 μM). Notably, compound **24** with 2,4-bis(trifluoromethyl)benzyl showed the most potent and broad inhibitory activities against DENV-1 to -3 with EC_{50} values of 1.6 μM, 0.038 μM and 0.017 μM, respectively. Unfortunately, all these compounds did not show obvious inhibitory activities against DENV-4 at the concentration up to 5 μM.

Next, we turned to explore the SAR around the pyrazolopyridone core. These modifications, as shown in Scheme 1–3, yielded compounds **25-32** (Table 2). To this end, compounds **25-28** were prepared in a similar manner to that described above for compounds **16-24**. Benzylation of aminopyrazole derivatives **4a-c** was followed by a three-component condensation to afford derivatives **25–28** (Scheme 1). Cyclization of succinonitrile, ethyl formate and 4-chlorobenzylamine provided aminopyrrole **34** via multiple procedures, which was then treated with 5-chloroisatin and Meldrum's acid to produce spiropyrrolopyridone **29** (Scheme 2). Substitution of 4-chlorobenzyl chloride with hydrazine provided substituted hydrazine **36**, which was condensed with (*E*)-ethyl 2-cyano-3-ethoxyacrylate to give aminocarboxylate **37**. Hydrolysis of ester **37** gave the sodium salt, which was directly used for the subsequent three component reaction with Meldrum's and ethyl acetoacetate or methyl cyanoacetate or methyl malonamate to yield derivatives **30-32**, respectively (Scheme 3). The structures and purity of all synthesized compounds were confirmed by ^{1}H and ^{13}C NMR, HR-MS and HPLC analysis.[29]

As shown in Table 2, moving the benzyl chains to the adjacent nitrogen position (**25** and **26**) led to a sharp decrease in activity against DENV-2 in comparison with compounds **1** and **21**, respectively. Interestingly, introduction of one methyl group at the 3′-site of the pyrazolopyridone core (**27**) retained the same level of potency against DENV-1 (EC_{50} = 2.5 μM) and DENV-3 (EC_{50} = 0.025 μM) while diminishing the antiviral activity against DENV-2 (EC_{50} = 1.8 μM) in contrast to compound **1**. Substitution of 3′-methyl of compound **27** with 3′-cyclopropyl produced compound **28** with similar potency against DENV-2 (EC_{50} = 1.9 μM). Compound **29** with 3′-cyano pyrrolopyridone core were inactive against DENV-2 up to 5 μM. The 5′-position of the pyrazolopyridone core (α-carbonyl carbon) was also investigated and introduction of different substituents yielded compounds **30-32.** These changes resulted in a dramatic loss in activities against DENV-2, and only compound **32** with carbamoyl moiety exhibited low micromolar potency against DENV-2 with an EC_{50} value of 3.2 μM.

In summary, a series of spiropyrazolopyridone derivatives was synthesized to explore the SAR around the pyrazolopyridone core. Introducing different substituents at the 3′- or 5′-site or moving the benzyl chain to the adjacent nitrogen led to a significant loss of potency on DENV-2. While a narrow range of substitutions were tolerated at the *para*-position of the phenyl ring, di-substitution on the phenyl ring is beneficial for DENV-2 potency and has variable influences on DENV-3 potency depending on the exact compound. Among these molecules, while compounds **22** (**JMX0376**) and **24** (**JMX0395**) displayed similar potency profiles, compound **24** with 2,4-bis(trifluoromethyl)benzyl showed the most potent and broadest inhibitory activities against DENV-1 to -3 with EC_{50} values of 1.6 μM, 0.038 μM and 0.017 μM, respectively.

Acknowledgments

This work was supported by the John S. Dunn Foundation, the Amon G. Carter Foundation, the Kleberg Foundation, the Gilson Longenbaugh Foundation, the Summerfield Robert Foundation, CDC grant U01CK0000512, NIH grants U19AI142759, 1R41AI136126, and R01AI127744, John Sealy Memorial Endowment Fund, John D. Stobo, M.D. Distinguished Chair Endowment Fund, and Institute for Translational Sciences (ITS) at UTMB.

References and notes

1. Dengue Guidelines for Diagnosis, Treatment, Prevention and Control : New Edition. World Health Organization: Geneva. 2009.
2. Brady OJ; Gething PW; Bhatt S, et al. Refining the global spatial limits of dengue virus transmission by evidence-based consensus. PLoS Negl Trop Dis. 2012; 6(8): e1760. [PubMed: 22880140]
3. Jentes ES; Lash RR; Johansson MA, et al. Evidence-based risk assessment and communication: a new global dengue-risk map for travellers and clinicians. J Travel Med. 2016; 23(6): taw062. [PubMed: 27625400]
4. Global Strategy for Dengue Prevention and Control, 2012–2020. World Health Organization: Geneva. 2012.
5. Bhatt S; Gething PW; Brady OJ, et al. The global distribution and burden of dengue. Nature. 2013; 496(7446): 504. [PubMed: 23563266]
6. Stanaway JD; Shepard DS; Undurraga EA, et al. The global burden of dengue: an analysis from the Global Burden of Disease Study 2013. Lancet Infect Dis. 2016; 16(6): 712. [PubMed: 26874619]
7. Montoya M; Gresh L; Mercado JC, et al. Symptomatic versus inapparent outcome in repeat dengue virus infections is influenced by the time interval between infections and study year. PLoS Negl Trop Dis. 2013; 7(8): e2357. [PubMed: 23951377]
8. Reich NG; Shrestha S; King AA, et al. Interactions between serotypes of dengue highlight epidemiological impact of cross-immunity. J R Soc Interface. 2013; 10(86): 20130414. [PubMed: 23825116]
9. Gubler DJ Dengue and dengue hemorrhagic fever. Clin Microbiol Rev. 1998; 11(3): 480. [PubMed: 9665979]
10. Halstead SB, O'Rourke EJ Antibody-enhanced dengue virus infection in primate leukocytes. Nature. 1977; 265(5596): 739. [PubMed: 404559]
11. Guzman MG; Alvarez M, Halstead SB Secondary infection as a risk factor for dengue hemorrhagic fever/dengue shock syndrome: an historical perspective and role of antibody-dependent enhancement of infection. Arch Virol. 2013; 158(7): 1445. [PubMed: 23471635]
12. Endy TP; Yoon IK, Mammen MP Prospective cohort studies of dengue viral transmission and severity of disease. Curr Top Microbiol Immunol. 2010; 338: 1. [PubMed: 19802574]
13. Vannice KS; Wilder-Smith A; Barrett ADT, et al. Clinical development and regulatory points for consideration for second-generation live attenuated dengue vaccines. Vaccine. 2018; 36(24): 3411. [PubMed: 29525283]
14. Global Advisory Committee on Vaccine Safety, 6–7 June 2018. Weekly Epidemiological Record. World Heathl Organization: Geneva. 2018; Vol. 93 (29/30): pp 388–396.
15. Villar L; Dayan GH; Arredondo-García JL, et al. Efficacy of a Tetravalent Dengue Vaccine in Children in Latin America. N Engl J Med. 2014; 372(2): 113. [PubMed: 25365753]
16. Dengue Vaccine: WHO Position Paper-September 2018. Weekly Epidemiological Record. World Health Organization: Geneva. 2018; Vol. 93: pp 457–476.
17. Behnam MAM; Nitsche C; Boldescu V, Klein CD The medicinal chemistry of dengue virus. J Med Chem. 2016; 59(12): 5622. [PubMed: 26771861]
18. Zou B; Chan WL; Ding M, et al. Lead optimization of spiropyrazolopyridones: a new and potent class of dengue virus inhibitors. ACS Med Chem Lett. 2015; 6(3): 344. [PubMed: 25878766]
19. Wang Q-Y; Dong H; Zou B, et al. Discovery of dengue virus NS4B inhibitors. J Virol. 2015; 89(16): 8233. [PubMed: 26018165]
20. Ye N; Chen H; Wold EA; Shi P-Y, Zhou J Therapeutic potential of spirooxindoles as antiviral agents. ACS Infect Dis. 2016; 2(6): 382. [PubMed: 27627626]
21. Xu J; Xie X; Ye N, et al. Design, synthesis, and biological evaluation of substituted 4,6-dihydrospiro[[1,2,3]triazolo[4,5-b]pyridine-7,3'-indoline]-2',5(3H)-dione analogues as potent NS4B inhibitors for the treatment of dengue virus infection. J Med Chem. 2019; 62(17): 7941. [PubMed: 31403780]
22. Fan X; Xu J; Files M, et al. Dual activity of niclosamide to suppress replication of integrated HIV-1 and Mycobacterium tuberculosis (Beijing). Tuberculosis (Edinb). 2019; 116: 28.

23. Niu Q; Liu Z; Alamer E, et al. Structure-guided drug design identifies a BRD4-selective small molecule that suppresses HIV. J Clin Invest. 2019; 129(8): 3361. [PubMed: 31329163]

24. Xu J; Berastegui-Cabrera J; Chen H; Pachón J; Zhou J, Sanchez-Cespedes J Structure-activity relationship studies on diversified salicylamide derivatives as potent inhibitors of human adenovirus infection. J Med Chem. 2020; 63(6): 3142. [PubMed: 32045239]

25. Li Z; Brecher M; Deng Y-Q, et al. Existing drugs as broad-spectrum and potent inhibitors for Zika virus by targeting NS2B-NS3 interaction. Cell Res. 2017; 27(8): 1046. [PubMed: 28685770]

26. Xu J; Shi P-Y; Li H, Zhou J Broad spectrum antiviral agent niclosamide and its therapeutic potential. ACS Infect Dis. 2020: 10.1021/acsinfecdis.0c00052.

27. General procedures for synthesizing the final products (exemplified by compound 21). To a solution of 3-aminopyrazole (330 mg, 3.97 mmol) in 8 mL of DMF was added NaH (238 mg, 5.96 mmol, 60% dispersion in mineral oil) at 0 °C. After addition, the mixture was stirred at 50 °C for 1 h. Then the mixture was cooled to r.t. and 4-(bromomethyl)-1,2-dichlorobenzene (1.43 g, 5.96 mmol) was added. The resulting mixture was stirred at r.t. for 2 h. Then the mixture was diluted with 120 mL of EtOAc, washed with water (2 × 30 mL) and brine (30 mL), dried (Na_2SO_4) and concentrated. The residual was purified by column chromatography (Hex/EtOAc = 2/1 to 1/1) to give the amino intermediate 1-(3,4-dichlorobenzyl)-1*H*-pyrazol-5-amine **9a** (105 mg, 11%) as yellow oil. ^{1}H NMR (300 MHz, $CDCl_3$) δ 7.39 (d, *J* = 8.1, 1H), 7.33 (d, *J* = 1.8 Hz, 1H), 7.24 (d, *J* = 1.8 Hz, 1H), 6.99 (dd, *J* = 8.4, 2.1 Hz, 1H), 5.61 (d, *J* = 1.8 Hz, 1H), 5.15 (s, 2H), 3.38 (s, 2H). A solution of aminopyrazole **9a** (105 mg, 0.43 mmol), 5-chloroisatin (86 mg, 0.48 mmol) and Meldrum's acid (94 mg, 0.65 mmol) in 2 mL of AcOH was stirred at 100 °C for 12 h. The reaction mixture was cooled to r.t. and concentrated *in vacuo*. The residue was stirred with water (10 mL) for 15 min. And the solid precipitate was filtered and further purified by column chromatography (DCM/MeOH = 30/1 to 20/1) to give 5-chloro-1'-(3,4-dichlorobenzyl)-5',7'-dihydrospiro[indoline-3,4'-pyrazolo[3,4-b]pyridine]-2,6'(1'*H*)-dione (**21**) as a yellow solid (90 mg, 46%). HPLC purity 99.7% (t_R = 16.91 min). ^{1}H NMR (300 MHz, DMSO-d_6) δ 11.08 (s, 1H), 10.60 (s, 1H), 7.64 (d, *J* = 8.4 Hz, 1H), 7.51 (d, *J* = 1.8 Hz, 1H), 7.35 – 7.27 (m, 2H), 7.21 (dd, *J* = 8.4, 1.8 Hz, 1H), 6.91 (d, *J* = 8.4 Hz, 1H), 6.83 (s, 1H), 5.32 (d, *J* = 15.9 Hz, 1H), 5.25 (d, *J* = 15.9 Hz, 1H), 3.13 (d, *J* = 15.9 Hz, 1H), 2.57 – 2.51 (m, 1H). 13C NMR (75 MHz, DMSO-d_6) δ 178.4, 168.8, 140.8, 140.5, 137.9, 134.6, 133.7, 131.0, 130.8, 130.3, 129.6, 128.7, 128.0, 126.1, 124.0, 111.3, 100.4, 49.5, 45.8. HRMS (ESI) calcd for $C_{20}H_{14}Cl_3N_4O_2$, 447.0182 $(M + H)^+$; found, 447.0180.

28. Luciferase Reporter Replicon-Based Screening. Huh7 cells containing a luciferase reporter replicon of DENV-1 (strain WestPac), DENV-2 (New Guinea C strain, NGC), DENV-3 (strain D3MY05-34640) and DENV-4 (strain D4MY01-22713) were used in this study. The replicon cells containing the Renilla luciferase and neomycin-resistance genes were generated using a similar strategy as described previously (EBioMedicine. 2016, 12, 156–160. doi: 10.1016/j.ebiom.2016.09.013). Briefly, Huh7 DENV-1 to -4 replicon cells were seeded at a density of 10k per well in a 96-well microplate. After incubation at 37 °C with 5% CO_2 overnight, the cells were treated with 2-fold serial dilutions of compounds. Experiments were performed in duplicates. After 48 h of incubation, luciferase activities were measured using the EnduRen live-cell substrate (Promega) by following the manufacture's instructions. Following luciferase activity measurement, the CellTiter-Glo reagent (Promega) was added to each well to determine the cytotoxicity of the compounds. The dose-dependent curve was plotted and EC_{50} values were calculated using four parameter logistic regression in GraphPad software Prism 8.0. [PubMed: 27658737] $_{250}$

29. Spectra data of other representative compounds: 5-Chloro-1'-(4-chloro-3-fluorobenzyl)-5',7'-dihydrospiro[indoline-3,4'-pyrazolo[3,4-*b*]pyridine]-2,6'(1'*H*)-dione (**22**). Yellow solid. HPLC purity 98.9% (t_R = 16.41 min). ^{1}H NMR (300 MHz, DMSO-d_6) δ 11.07 (s, 1H), 10.60 (s, 1H), 7.59 (t, *J* = 8.1 Hz, 1H), 7.34 – 7.27 (m, 2H), 7.24 (dd, *J* = 10.2, 1.8 Hz, 1H), 7.08 (dd, *J* = 8.4, 1.5 Hz, 1H), 6.91 (d, *J* = 8.1 Hz, 1H), 6.82 (s, 1H), 5.34 (d, *J* = 16.2 Hz, 1H), 5.27 (d, *J* = 15.9 Hz, 1H), 3.13 (d, *J* = 15.9 Hz, 1H), 2.57 – 2.50 (m, 1H). ^{13}C NMR (75 MHz, DMSO-d_6) δ 178.4, 168.8, 157.0 (d, *J* = 245.3 Hz), 140.8, 140.5, 138.6 (d, *J* = 6.6 Hz), 134.5, 133.7, 130.8, 128.6, 126.1, 124.8 (d, *J* = 3.5 Hz), 124.0, 118.6 (d, *J* = 17.3 Hz), 115.9 (d, *J* = 21.4 Hz), 111.3, 100.4, 49.7, 45.8. HRMS (ESI) calcd for $C_{20}H_{14}Cl_2FN_4O_2$, 431.0478 $(M + H)^+$; found, 431.0476. 5-Chloro-1'-(4-chloro-2-fluorobenzyl)-5',7'-dihydrospiro[indoline-3,4'-

pyrazolo[3,4-*b*]pyridine]-2,6'(1'*H*)-dione (**23**). Yellow solid. HPLC purity 95.9% (t_R = 17.26 min). ^{1}H NMR (300 MHz, DMSO-d_6) δ 11.07 (s, 1H), 10.59 (s, 1H), 7.47 (dd, *J* = 9.9, 1.8 Hz, 1H), 7.37 – 7.24 (m, 3H), 7.07 (t, *J* = 8.1 Hz, 1H), 6.91 (d, *J* = 7.8 Hz, 1H), 6.80 (s, 1H), 5.38 (d, *J* = 15.9 Hz, 1H), 5.29 (d, *J* = 15.9 Hz, 1H), 3.12 (d, *J* = 15.9 Hz, 1H), 2.54 (d, *J* = 15.9 Hz, 1H). ^{13}C NMR (75 MHz, DMSO-d_6) δ 178.4, 168.7, 159.7 (d, *J* = 248.5 Hz), 140.8, 140.7, 134.5, 133.7, 133.2 (d, *J* = 10.3 Hz), 130.8 (d, *J* = 5.1 Hz), 128.6, 126.1, 124.8 (d, *J* = 3.6 Hz), 124.0, 123.2 (d, *J* = 14.9 Hz), 116.0 (d, *J* = 24.8 Hz), 111.3, 100.3, 45.8, 44.7. HRMS (ESI) calcd for $C_{20}H_{14}Cl_2FN_4O_2$, 431.0478 (M + H)$^+$; found, 431.0474. 1'-(2,4-Bis(trifluoromethyl)benzyl)-5-chloro-5',7'-dihydrospiro[indoline-3,4'-pyrazolo[3,4-*b*]pyridine]-2,6'(1'*H*)-dione (**24**). Yellow solid. HPLC purity 97.9% (t_R = 18.63 min). 1H NMR (300 MHz, CD_3OD + $CDCl_3$) δ 7.94 (s, 1H), 7.80 (d, *J* = 8.1 Hz, 1H), 7.26 (dd, *J* = 8.4, 2.1 Hz, 1H), 7.20 (d, *J* = 1.8 Hz, 1H), 6.99 (s, 1H), 6.92 (d, *J* = 8.4 Hz, 1H), 6.84 (d, *J* = 8.4 Hz, 1H), 5.64 (d, *J* = 17.7 Hz, 1H), 5.56 (d, *J* = 17.7 Hz, 1H), 2.96 (d, *J* = 16.2 Hz, 1H), 2.80 (d, *J* = 16.2 Hz, 1H). ^{13}C NMR (75 MHz, CD_3OD + $CDCl_3$) δ 180.0, 170.3, 142.5, 140.6, 139.9, 136.5, 133.7, 130.9 (q, *J* = 33.5 Hz), 130.1 – 129.9 (m), 129.9, 129.0, 128.9, 128.6 (q, *J* = 32.0 Hz), 124.5, 124.1 (q, *J* = 272.2 Hz), 124.0 – 123.6 (m), 123.8 (q, *J* = 270.4 Hz), 112.2, 101.9, 48.5 (q, *J* = 3.9 Hz), 47.0, 41.1. HRMS (ESI) calcd for $C_{22}H_{14}ClF_6N_4O_2$, 515.0709 (M + H)$^+$; found, 515.0707. 5-Chloro-1'-(4-chlorobenzyl)-3'-methyl-5',7'-dihydrospiro[indoline-3,4'-pyrazolo[3,4-*b*]pyridine]-2,6'(1'*H*)-dione (**27**). Yellow solid. HPLC purity 96.7% (t_R = 17.19 min). 1H NMR (300 MHz, DMSO-d_6) δ 11.02 (s, 1H), 10.66 (s, 1H), 7.46 – 7.38 (m, 2H), 7.33 – 7.28 (m, 2H), 7.27 – 7.21 (m, 2H), 6.95 – 6.89 (m, 1H), 5.23 (d, *J* = 15.9 Hz, 1H), 5.16 (d, *J* = 15.9 Hz, 1H), 3.05 (d, *J* = 15.9 Hz, 1H), 2.59 (d, *J* = 15.9 Hz, 1H), 1.42 (s, 3H). 13C NMR (75 MHz, DMSO-d_6) δ 178.2, 168.6, 142.6, 140.6, 140.6, 136.1, 133.5, 132.1, 129.4 (2C), 128.6, 128.5 (2C), 126.0, 124.0, 111.3, 97.1, 49.6, 46.1, 11.8. HRMS (ESI) calcd for $C_{21}H_{17}Cl_2N_4O_2$, 427.0729 (M + H)$^+$; found, 427.0725.

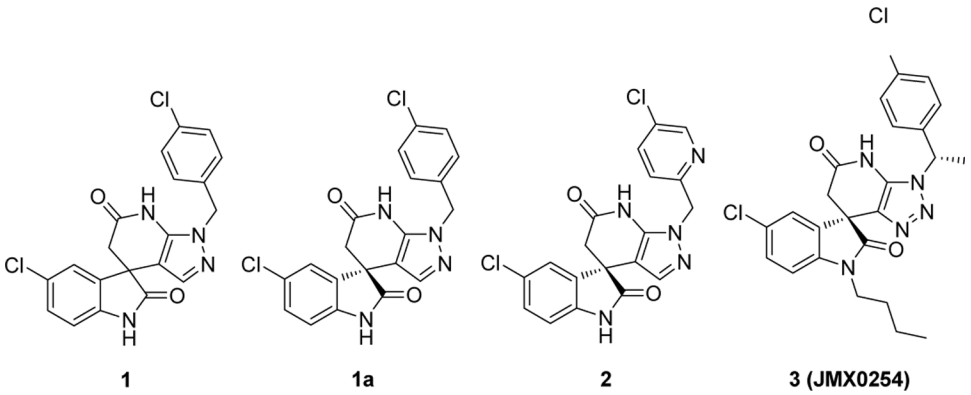

Figure 1.
The previously reported spiropyrazolopyridone derivatives as potent dengue virus inhibitors.

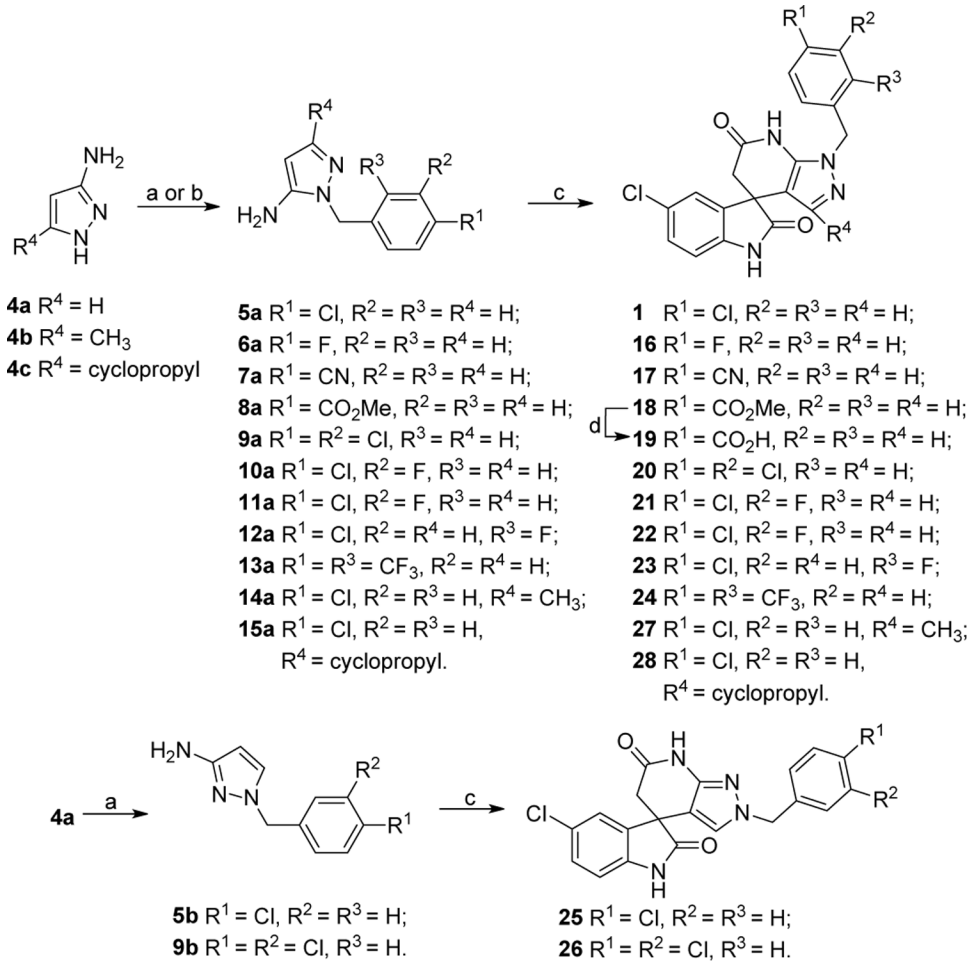

4a R^4 = H
4b R^4 = CH_3
4c R^4 = cyclopropyl

5a R^1 = Cl, R^2 = R^3 = R^4 = H;
6a R^1 = F, R^2 = R^3 = R^4 = H;
7a R^1 = CN, R^2 = R^3 = R^4 = H;
8a R^1 = CO_2Me, R^2 = R^3 = R^4 = H;
9a R^1 = R^2 = Cl, R^3 = R^4 = H;
10a R^1 = Cl, R^2 = F, R^3 = R^4 = H;
11a R^1 = Cl, R^2 = F, R^3 = R^4 = H;
12a R^1 = Cl, R^2 = R^4 = H, R^3 = F;
13a R^1 = R^3 = CF_3, R^2 = R^4 = H;
14a R^1 = Cl, R^2 = R^3 = H, R^4 = CH_3;
15a R^1 = Cl, R^2 = R^3 = H, R^4 = cyclopropyl.

1 R^1 = Cl, R^2 = R^3 = R^4 = H;
16 R^1 = F, R^2 = R^3 = R^4 = H;
17 R^1 = CN, R^2 = R^3 = R^4 = H;
18 R^1 = CO_2Me, R^2 = R^3 = R^4 = H;
19 R^1 = CO_2H, R^2 = R^3 = R^4 = H;
20 R^1 = R^2 = Cl, R^3 = R^4 = H;
21 R^1 = Cl, R^2 = F, R^3 = R^4 = H;
22 R^1 = Cl, R^2 = F, R^3 = R^4 = H;
23 R^1 = Cl, R^2 = R^4 = H, R^3 = F;
24 R^1 = R^3 = CF_3, R^2 = R^4 = H;
27 R^1 = Cl, R^2 = R^3 = H, R^4 = CH_3;
28 R^1 = Cl, R^2 = R^3 = H, R^4 = cyclopropyl.

5b R^1 = Cl, R^2 = R^3 = H;
9b R^1 = R^2 = Cl, R^3 = H.

25 R^1 = Cl, R^2 = R^3 = H;
26 R^1 = R^2 = Cl, R^3 = H.

Scheme 1.

Synthetic route of compounds **16-28**. Reagents and conditions: (a) NaH, various substituted benzyl bromide or benzyl chloride, DMF, 0 °C to r.t., 12 h, **5a-14a**, **5b** and **9b**. (b) K_2CO_3, 4-chlorobenzyl chloride, CH_3CN, 60 °C, 12 h, **15a**. (c) 5-chloroisatin, Meldrum's acid, AcOH, 100 °C, 12 h. (d) NaOH, MeOH/H_2O, r.t., 2 h.

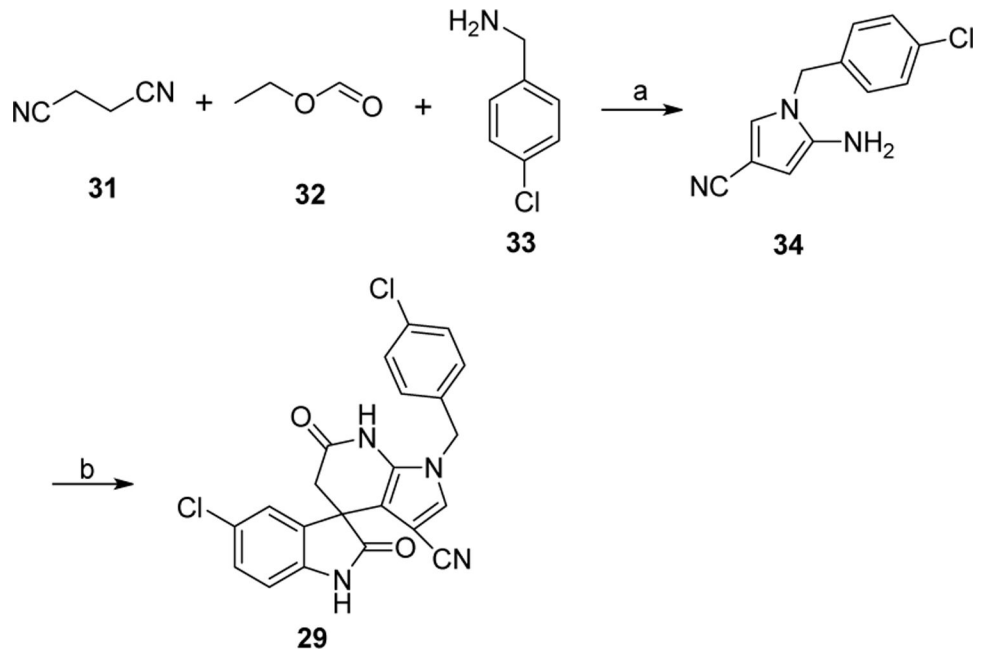

Scheme 2.

Synthetic route of compound **29**. Reagents and conditions: (a) i. *t*-KOBu, THF, 0 °C to r.t., 30 min; ii. H_2O, r.t.; iii. AcOH, 100 °C, 10 min; iv. NaOEt, EtOH, r.t., 60 min. (b) 5-chloroisatin, Meldrum's acid, NH_4OAc, AcOH, 100 °C, 12 h.

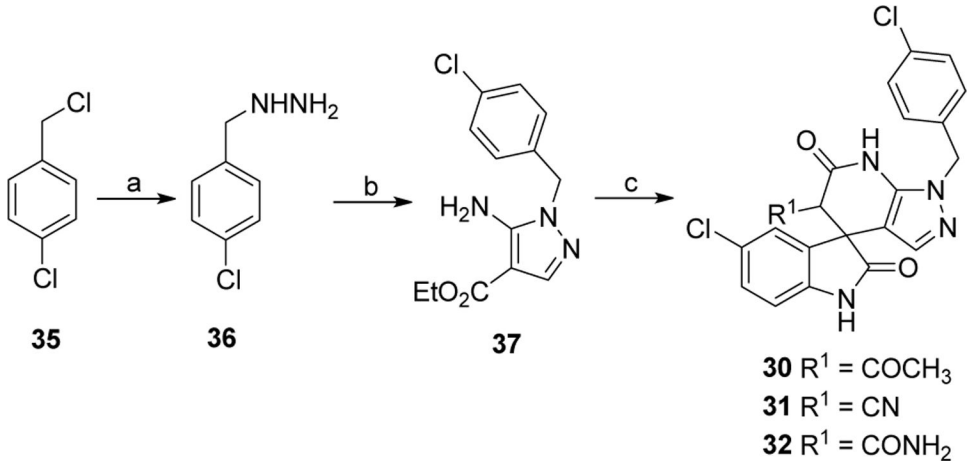

Scheme 3.

Synthetic route of compounds **30–32**. Reagents and conditions: (a) $N_2H_4 \cdot H_2O$, EtOH, r.t., 48 h. (b) (*E*)-ethyl 2-cyano-3-ethoxyacrylate, EtOH, 80 °C, 8 h. (c) i. NaOH, EtOH/H_2O, reflux, overnight; ii. 5-chloroisatin, ethyl acetoacetate or methyl cyanoacetate or methyl malonamate, AcOH, 100 °C, 6 h.

Table 1.

Antiviral Activity and Cytotoxicity of Compounds 16–24[a]

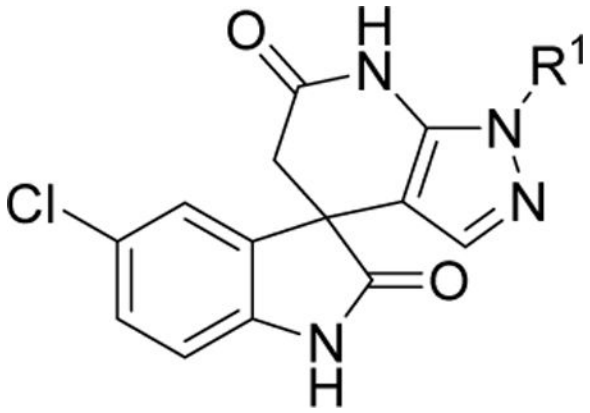

Compd	R[1]	EC$_{50}$ (μM)				CC$_{50}$(μM)
		D-1	D-2	D-3	D-4	
1	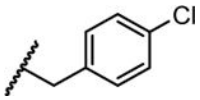	2.4	0.11	0.006	>10	>10
16	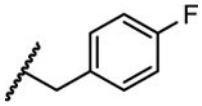	NT	4.2	NT	NT	NT
17	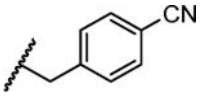	NT	>5	NT	NT	NT
18	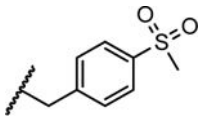	NT	>5	NT	NT	NT
19	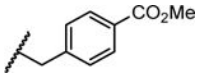	NT	>5	NT	NT	NT
20	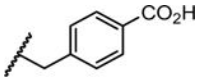	NT	>5	NT	NT	NT
21	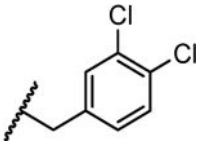	1.8	0.062	>5	>5	>10

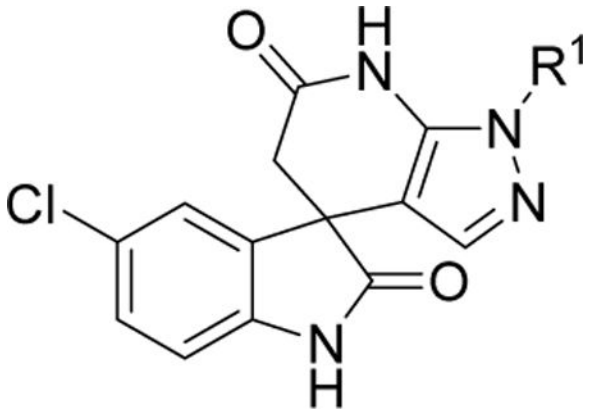

Compd	R[1]	EC$_{50}$ (μM)				CC$_{50}$(μM)
		D-1	D-2	D-3	D-4	
22	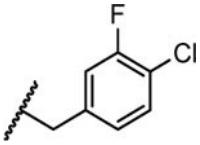	1.8	0.050	0.019	>5	>10
23	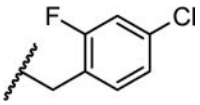	2.3	0.14	0.39	>5	>10
24	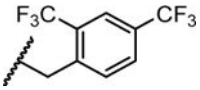	1.6	0.038	0.017	>5	>10

[a]EC$_{50}$ values were determined on Huh7 cells stably expressing DENV-1 to -4 replicon; CC$_{50}$ values were measured using Huh7 cells stably expressing DENV-2 replicon; D-1: DENV-1; D-2: DENV-2; D-3: DENV-3; D-4: DENV-4; NT: not tested.

Table 2.

Antiviral Activity and Cytotoxicity of Compounds **25–32**[a]

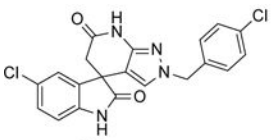

25

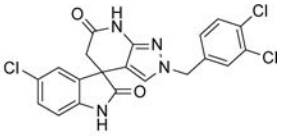

26

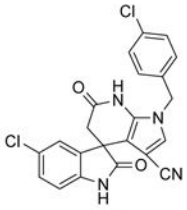

29

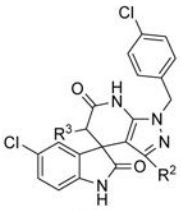

27-28, 30-32

Compd	R^2	R^3	EC_{50} (μM)				CC_{50}(μM)
			D-1	D-2	D-3	D-4	
25			NT	4.4	NT	NT	>10
26			NT	1.1	NT	NT	>10
27	CH_3	H	2.5	1.8	0.025	>5	>10
28		H	NT	1.9	NT	NT	>10
29			NT	>5	NT	NT	NT
30	H		NT	>10	NT	NT	>20
31	H	CN	NT	8.6	NT	NT	50
32	H		NT	3.2	NT	NT	50

[a] EC_{50} values were determined on Huh7 cells stably expressing DENV-1 to -4 replicon; CC_{50} values were measured using Huh7 cells stably expressing DENV-2 replicon; D-1: DENV-1; D-2: DENV-2; D-3: DENV-3; D-4: DENV-4; NT: not tested.